


## Dissipation-recurrence inequalities at the steady state

Diego Frezzato <sup>\*</sup>

*Department of Chemical Sciences, University of Padova, Via Marzolo 1, 35131 Padova, Italy*

 (Received 17 December 2020; revised 15 February 2021; accepted 16 February 2021; published 10 March 2021)

For Markov jump processes in out-of-equilibrium steady state, we present inequalities which link the average rate of entropy production with the timing of the site-to-site recurrences. Such inequalities are upper bounds on the average rate of entropy production. The combination with the finite-time thermodynamic uncertainty relation (a lower bound) yields inequalities of the pure kinetic kind for the relative precision of a dynamical output. After having derived the main relations for the discrete case, we sketch the possible extension to overdamped Markov dynamics on continuous degrees of freedom, treating explicitly the case of one-dimensional diffusion in tilted periodic potentials; an upper bound on the average velocity is derived, in terms of the average rate of entropy production and the microscopic diffusion coefficient, which corresponds to the finite-time thermodynamic uncertainty relation in the limit of vanishingly small observation time.

DOI: [10.1103/PhysRevE.103.032112](https://doi.org/10.1103/PhysRevE.103.032112)

### I. INTRODUCTION

For thermostated fluctuating systems in out-of-equilibrium steady states (maintained due to external persistent actions such as enforcement of chemostats, coupling with chemical reactions, and interaction with radiation) it is known that the average rate of entropy production  $\sigma^{\text{ss}}$  controls various features such as speed and precision of events of interest. We mention the variety of thermodynamic uncertainty relations (see, for instance, the central works [1,2]) and the recent interest in dissipation-time uncertainty relations [3] for the minimum time required to complete a certain operation.

In this work we inspect a different facet of the connection between  $\sigma^{\text{ss}}$  and the timescale of the internal system's dynamics. We mainly work within the setup of stationary Markov jump processes in which the discrete state space forms a network with a finite number of sites and constant site-to-site jump rates; the extension to continuous degrees of freedom with diffusive dynamics is sketched later. For each pair of connected sites, the repetition of the site-to-site jump is a sort of clock signal which occurs with an average recurrence frequency. Here we investigate how such average frequencies are interrelated with  $\sigma^{\text{ss}}$  [Eqs. (6)–(9)] and with a suitably defined mean current [Eq. (13)] in out-of-equilibrium steady-state conditions. The target is to derive inequalities and make statements involving a small amount of information about the system. As a side product, inequalities of a purely kinetic kind [Eqs. (14) and (15)] are obtained by combining the upper bounds on  $\sigma^{\text{ss}}$ , derived herein, with the lower bound expressed by the finite-time thermodynamic uncertainty relation [1,2].

Let us consider a network with  $N$  sites and let  $k_{i \rightarrow j}$  be the jump rate from  $i$  to  $j$ . Let us assume that the site-to-site transitions are elementary (undecomposable) processes and, for thermodynamic consistency, assume that if  $i \rightarrow j$  can

take place, also the reversed transition  $j \rightarrow i$  is allowed. By indicating with  $p_i^{\text{ss}}$  the steady-state probability of occupying site  $i$ , the average rate of entropy production (here in units of the Boltzmann constant  $k_B$ ) [4]

$$\sigma^{\text{ss}} = \sum_i \sum_{j < i} (p_j^{\text{ss}} k_{j \rightarrow i} - p_i^{\text{ss}} k_{i \rightarrow j}) \ln \frac{p_j^{\text{ss}} k_{j \rightarrow i}}{p_i^{\text{ss}} k_{i \rightarrow j}} \quad (1)$$

quantifies the deviation of the steady state from equilibrium in terms of the extent of the detailed-balance breakdown (in fact,  $\sigma^{\text{ss}}$  is non-negative and null only if the balancing  $p_j^{\text{ss}} k_{j \rightarrow i} = p_i^{\text{ss}} k_{i \rightarrow j}$  is fulfilled for all pairs of connected sites). Note that, for thermostated systems, talk of the average rate of entropy production (in  $k_B$  units) or of energy dissipated as heat (in  $k_B T$  units) is equivalent.

If we take a pair of connected sites, say,  $i$  and  $j$ , and if the jump  $i \rightarrow j$  has just occurred, we may ask what the wait time  $\tau_{ij}$  is for observing that jump again. The stochastic nature of the dynamics (both the system's path among the sites and the times at which the transitions take place are aleatory) makes  $\tau_{ij}$  be distributed. Here  $\bar{\tau}_{ij}$  is the average time over the distribution, and its inverse  $\bar{\omega}_{ij} = \bar{\tau}_{ij}^{-1}$  is interpreted as the average recurrence frequency of the  $i \rightarrow j$  transition. The relative precision of the recurrence can be quantified, for instance, by the squared coefficient of variation  $(\overline{\tau_{ij}^2} - \bar{\tau}_{ij}^2)/\bar{\tau}_{ij}^2$  [5].

Based on the fact that  $\bar{\tau}_{ij}^{-1} = p_i^{\text{ss}} k_{i \rightarrow j}$  [5], it has been recently pointed out that  $\sigma^{\text{ss}}$  in Eq. (1) can be rewritten on the basis of the full set  $\{\bar{\tau}_{ij}\}$ ; in terms of the average recurrence frequencies, it reads

$$\sigma^{\text{ss}} = \sum_i \sum_{j < i} (\bar{\omega}_{ji} - \bar{\omega}_{ij}) \ln \frac{\bar{\omega}_{ji}}{\bar{\omega}_{ij}}. \quad (2)$$

While the form of  $\sigma^{\text{ss}}$  in Eq. (1) contains quantities of mixed nature, namely, statistical populations and jump rates, Eq. (2) contains only pure kinetic quantities (although of the

<sup>\*</sup>diego.frezzato@unipd.it

statistical kind since we deal with *average* recurrence frequencies). Although such a change of representation might seem little, it is the starting point for deriving inequalities in which  $\sigma^{\text{ss}}$  is connected with the dynamical behavior of the system.

As stated above, we will focus first on the discrete case with a finite number of sites. It must be stressed that the discrete case not only simplifies the mathematics (possibly taking then the continuum limit), but also pertains to several processes of physical relevance. Besides the cases in which the state space is intrinsically discrete, the discreteness comes into play also when a coarse-graining procedure allows one to work out an approximate but effective jump process. Many examples are found in the (bio)chemical ambit [6], such as the conformational dynamics of complex molecules [7], discrete models of molecular motors and directed motion under nonequilibrium conditions [8,9], stochastic chemical kinetics in the configurational space of the molecule copy numbers [10], and jumps of a tagged molecular moiety from species to species due to the occurrence of chemical reactions [11,12]. The results that we are going to present can thus be applied to a wealth of processes.

At a subsequent level, we move the first steps in the application of the general results to the dynamics on continuous degrees of freedom which, upon discretization, can be cast in the form of a jump process among a finite number  $N$  of sites (then taking the limit  $N \rightarrow \infty$ ). We will consider the paradigmatic case of one-dimensional diffusion in a tilted potential, deriving an upper bound for the average velocity at the steady state in terms of the microscopic diffusion coefficient and  $\sigma^{\text{ss}}$ ; the result is Eq. (17) given later, which is nothing but the finite-time thermodynamic uncertainty relation [1,2] in the limit of vanishingly small observation time.

## II. SETUP AND NOTATION

Let us consider a network with  $N$  sites and  $N_c$  connections between them. A connection is here intended as a pair of forward and backward channels connecting two sites. For example, if we deal with  $N$  sites, all connected one with the others, then  $N_c = N(N-1)/2$ ; if the sites are connected in sequence forming a closed cycle, then  $N_c = N$ . In all generality there might be connections for which the forward and backward channels are balanced at the steady state (e.g., because of symmetry reasons in the network's topology) and so do not contribute to  $\sigma^{\text{ss}}$ . In what follows,  $N_c^* \leq N_c$  is the number of nonbalanced connections.

Under steady-state conditions, the dynamics of the site occupation probabilities  $p_i(t)$  is governed by the master equation  $\dot{\mathbf{p}} = -\mathbf{R}\mathbf{p}$ , where  $\mathbf{p}$  is the column array whose entries are the occupation probabilities and  $\mathbf{R}$  is the constant transition matrix having elements  $R_{ss'} = -k_{s' \rightarrow s}(1 - \delta_{s,s'}) + \delta_{s,s'} \sum_{n \neq s'} k_{s' \rightarrow n}$  (with  $\delta$  the Kronecker delta). For a generic transition  $i \rightarrow j$  between connected sites, the distribution of its recurrence time is given by  $\rho(\tau_{ij}) = k_{i \rightarrow j} p(i, \tau_{ij} \& \text{no } \mathcal{E}|j)$ , where  $\mathcal{E}$  stands for the event  $i \rightarrow j$  and  $p(i, t \& \text{no } \mathcal{E}|j)$  is the survival probability that if the system is initially at site  $j$  (and according to the Markovian assumption this is as if the event had just occurred), after time  $t$  it is found at site  $i$  (hence available for jumping to  $j$ ) and the event has not yet occurred. Such a conditioned

probability evolves according to a master equation with modified transition matrix  $\mathbf{K}$  whose elements are  $K_{ss'}(i \rightarrow j) = R_{ss'} + k_{i \rightarrow j} \delta_{s,j} \delta_{s',i}$ ; hence  $\rho(\tau_{ij}) = k_{i \rightarrow j} [e^{-\mathbf{K}(i \rightarrow j)\tau_{ij}}]_{ij}$ . As detailed in Refs. [5,11], the average recurrence time can be computed by means of

$$\bar{\tau}_{ij} = \sum_s [\mathbf{K}(i \rightarrow j)^{-1}]_{sj}, \quad (3)$$

which expresses the link between recurrence timing and jump rates. Let  $\bar{\tau}_{\text{max}}$  and  $\bar{\tau}_{\text{min}}$  be the longest and shortest average recurrence times, respectively:

$$\bar{\tau}_{\text{max}} = \max_{i,j} \{\bar{\tau}_{i,j}\}, \quad \bar{\tau}_{\text{min}} = \min_{i,j} \{\bar{\tau}_{i,j}\}. \quad (4)$$

Then

$$\bar{\omega}_{\text{min}} = \bar{\tau}_{\text{max}}^{-1}, \quad \bar{\omega}_{\text{max}} = \bar{\tau}_{\text{min}}^{-1} \quad (5)$$

are the associated average recurrence frequencies. These extrema depend on the size  $N$  of the network, on the site-to-site connections, and on the value of the jump rates. By considering again  $\bar{\tau}_{ij}^{-1} = p_i^{\text{ss}} k_{i \rightarrow j}$ , we can say that  $\bar{\omega}_{\text{max}}$  is surely upper bounded by  $\max_{i,j} \{k_{i \rightarrow j}\}$  and that  $\bar{\omega}_{\text{min}}$  takes a finite non-null value (because the values  $0 < p_i^{\text{ss}} < 1$  are possibly very small, but finite, for a network with a finite number of connected sites). Equivalently,  $\bar{\tau}_{\text{max}}$  is finite.

## III. DISSIPATION-RECURRENCE INEQUALITIES FOR JUMP PROCESSES

### A. Main results

An upper bound on  $\sigma^{\text{ss}}$  is readily obtained from Eq. (2) by considering that each addend is majorized upon replacing  $\bar{\omega}_{ji}$  with  $\omega_{\text{max}}$  and  $\bar{\omega}_{ij}$  with  $\bar{\omega}_{\text{min}}$ ; thus

$$\sigma^{\text{ss}} \leq N_c (\bar{\omega}_{\text{max}} - \bar{\omega}_{\text{min}}) \ln \frac{\bar{\omega}_{\text{max}}}{\bar{\omega}_{\text{min}}}. \quad (6)$$

By rearranging Eq. (6) we get

$$N_c (\epsilon - 1) \ln \epsilon \geq \sigma^{\text{ss}} \bar{\tau}_{\text{max}}, \quad (7)$$

with the spread  $\epsilon = \bar{\omega}_{\text{max}}/\bar{\omega}_{\text{min}} = \bar{\tau}_{\text{max}}/\bar{\tau}_{\text{min}}$ . It is worth stressing that while  $\sigma^{\text{ss}}$  is interpretable mainly thinking about an ensemble of independent system's replicas evolving in parallel, the quantity  $\sigma^{\text{ss}} \bar{\tau}_{\text{max}} = \sigma^{\text{ss}} \bar{\omega}_{\text{min}}^{-1}$  that appears in Eq. (7) (and other relations below) acquires a meaning also when referring to the individual system and expresses the statistical expectation about the net increase of entropy per repetition of the rarest recurrence. Given  $\sigma^{\text{ss}} \bar{\tau}_{\text{max}}/N_c$ , Eq. (7) sets a lower bound for the spread  $\epsilon$ .

By reversing the inequality (6) we get

$$\bar{\omega}_{\text{max}} \geq \bar{\omega}_{\text{min}} [1 + \gamma_{\uparrow}(\sigma^{\text{ss}} \bar{\omega}_{\text{min}}^{-1}/N_c)], \quad (8)$$

where the function  $\gamma_{\uparrow}(\cdot) \geq 1$  is such that, given  $y \geq 0$ ,  $\gamma_{\uparrow}(y)$  is the solution of the equation  $(x-1) \ln x = y$  for  $x \geq 1$ ; note that  $\gamma_{\uparrow}(0) = 1$  and  $\gamma_{\uparrow}(y)$  increases monotonically. On the basis of Eq. (8) we can state that, at fixed  $\bar{\omega}_{\text{min}}$  (i.e., at fixed longest average recurrence time), a network with small spread *can* be sustained only close enough to equilibrium. In particular, Eq. (8) allows us to make the following assertions.

*Statement 1.* Given  $\bar{\omega}_{\min}$  and  $\sigma^{\text{ss}}$ , there are surely average recurrence frequencies above the value  $\bar{\omega}_{\min}[1 + \gamma_{\uparrow}(\sigma^{\text{ss}}\bar{\omega}_{\min}^{-1}/N_c)]$ .

*Statement 2.* Given  $\bar{\omega}_{\min}$ , to ensure a spread  $\bar{\omega}_{\max}/\bar{\omega}_{\min}$  not less than  $\epsilon^*$ , the average rate of entropy production must be at least  $N_c\bar{\omega}_{\min}(\epsilon^* - 1)\ln\epsilon^*$ .

*Statement 3.* Given  $\bar{\omega}_{\min}$ , the spread  $\bar{\omega}_{\max}/\bar{\omega}_{\min}$  can be below  $\epsilon^*$  only if the average rate of entropy production is less than  $N_c\bar{\omega}_{\min}(\epsilon^* - 1)\ln\epsilon^*$ .

The relevance of general statements like these lies in the fact that they are formulated with very little information about the network. Note that the above inequalities and statements can be sharpened if one knows the number of balanced connections, if there are any, so that  $N_c$  can be replaced by  $N_c^*$ .

One may wish to find other bounds on  $\sigma^{\text{ss}}$ , possibly more stringent than Eq. (6), at least under certain conditions. With such a target in mind, the following inequality is derived from Eq. (2) by means of a multiple use of Jensen's inequality (the proof is provided in the Appendix)

$$\sigma^{\text{ss}} \leq 2N_c \langle \bar{\omega} \rangle_a \Phi\left(\frac{\bar{\omega}_{\max}}{\bar{\omega}_{\min}}\right), \quad (9)$$

where for the sake of compactness we have introduced the function

$$\Phi(\epsilon) = \left(\frac{\epsilon - 1}{\epsilon + 1}\right) \ln \epsilon \quad (10)$$

and where the quantity  $\langle \bar{\omega} \rangle_a$ , interpretable as a measure of system's "activity," is the arithmetic mean of the average recurrence frequencies [13],

$$\langle \bar{\omega} \rangle_a := \frac{1}{2N_c} \sum_i \sum_{j \neq i} \bar{\omega}_{ij}. \quad (11)$$

Like for Eq. (6), also the inequality (9) can be tightened by considering only the nonbalanced connections [see the more stringent form in Eq. (A16)]. By reversing Eq. (9) one obtains a lower bound on  $\langle \bar{\omega} \rangle_a$  in terms of  $\sigma^{\text{ss}}$  and spread  $\bar{\omega}_{\max}/\bar{\omega}_{\min}$ .

By comparing Eq. (6) with Eq. (9), one sees that Eq. (9) is more restrictive only if  $\langle \bar{\omega} \rangle_a < (\bar{\omega}_{\max} + \bar{\omega}_{\min})/2$ . Of course, the fulfillment of this condition depends on how the average recurrence frequencies are distributed between the extrema. Without doing the explicit calculation, it seems difficult to find a simple way to say which is the most stringent bound between Eqs. (6) and (9) given the connectivities and the values of the jump rates. However, at least for networks having rates randomly generated with uniform distribution on their logarithms in a given range (like in the simulations discussed below), it is found that Eq. (9) is typically more stringent than Eq. (6) and that the percentage of instances in which this happens rapidly increases with the number of sites. Of course one uses Eq. (6) or (9) depending on the information at disposal. If besides the spread  $\bar{\omega}_{\max}/\bar{\omega}_{\min}$  both  $\bar{\omega}_{\max}$  (or  $\bar{\omega}_{\min}$ ) and  $\langle \bar{\omega} \rangle_a$  are available,  $\sigma^{\text{ss}}$  is limited by the minimum between the two bounds.

It is important to stress that both Eqs. (6) and (9) are saturated under the same conditions (see the Appendix). Independently of how close to or far from equilibrium the steady state is, both relations become equalities in the special case in which all connections are nonbalanced ( $N_c^* = N_c$ ), and half

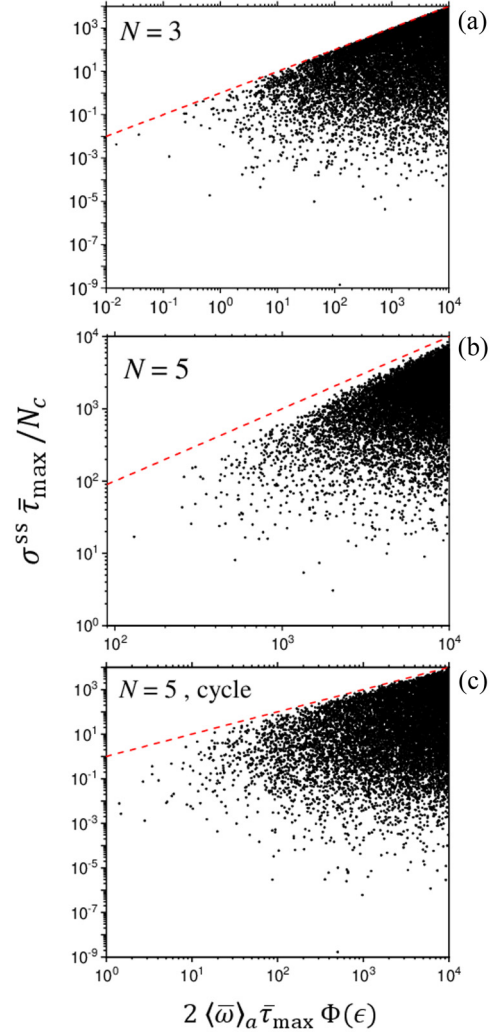


FIG. 1. Effectiveness of Eq. (9) for networks with (a)  $N = 3$  and (b) and (c)  $N = 5$  sites. For  $N = 3$  the sites (a) form a cycle, while for  $N = 5$  the sites (b) are all connected or (c) form a cycle. Each dot corresponds to a randomly generated instance (see Ref. [14]); each panel shows  $10^4$  instances. The dashed red lines have slope 1 and pass through the origin.

of the average recurrence frequencies are equal to  $\bar{\omega}_{\max}$  while the ones of the complementary backward processes are equal to  $\bar{\omega}_{\min}$ . For instance, this happens for peculiar realizations of sites connected forming a cycle (e.g., when all sites are equivalent with equal forward jump rates and equal backward jump rates). On the contrary, for arbitrary connection topologies, the right-hand sides of Eqs. (6) and (9) could be excessive majorizations of  $\sigma^{\text{ss}}$ . Note that Eqs. (6) and (9) hold also for detailed-balanced networks for which  $\sigma^{\text{ss}} = 0$ ; in such a case, however, the relations are trivial.

The effectiveness of Eq. (9) is illustrated in Fig. 1 for networks with  $N = 3$  and with  $N = 5$  sites. Each panel shows  $10^4$  instances with jump rates randomly generated; one rate was always set equal to 1 (just to fix an internal reference), while the other rates were varied randomly between  $10^{-4}$  and  $10^4$  [14]. For  $N = 3$  [Fig. 1(a)] all sites are of course connected forming a cycle. For  $N = 5$ , Fig. 1(b) refers to sites fully connected one with the others, while in Fig. 1(c) the sites

form a cycle. In all panels, the dashed line has slope 1 and passes through the origin; hence the fulfillment of the bound (9) corresponds to the population only of the area below the line. We can see that the inequality is indeed fulfilled and can be saturated if the sites are connected forming a cycle [note the change when passing from Fig. 1(b) to Fig. 1(c)]. For the instances in Fig. 1(a) it is found that Eq. (9) is more stringent than Eq. (6) in about 90% of the cases, and the percentage is nearly of 100% for the instances of Figs. 1(b) and 1(c).

Let us now introduce a mean out-of-equilibrium current and give upper and lower bounds on it. For a pair of connected sites  $i$  and  $j$ ,  $J_{i \rightarrow j}^{ss} = p_i^{ss} k_{i \rightarrow j} - p_j^{ss} k_{j \rightarrow i} \equiv \bar{\omega}_{ij} - \bar{\omega}_{ji}$  is the average current which expresses the net average number of jumps from  $i$  to  $j$  per unit of time, at the steady state, when thinking about a statistical ensemble of realizations;  $J_{j \rightarrow i}^{ss} = -J_{i \rightarrow j}^{ss}$ . In a detailed-balanced network all currents are null. Let us introduce the arithmetic mean of the average currents in modulus

$$\langle J^{ss} \rangle_a := \frac{1}{N_c^*} \sum_{i,j < i} |J_{i \rightarrow j}^{ss}| \quad (12)$$

and the mean frequency  $\langle \bar{\omega} \rangle'_a$  as the analog of Eq. (11) but evaluated only over the  $N_c^*$  nonbalanced connections. Is it proved (see the Appendix) that

$$\frac{\sigma^{ss}}{N_c \ln(\bar{\omega}_{\max}/\bar{\omega}_{\min})} \leq \langle J^{ss} \rangle_a \leq 2 \langle \bar{\omega} \rangle'_a g\left(\frac{\sigma^{ss}}{2N_c^* \langle \bar{\omega} \rangle'_a}\right), \quad (13)$$

where  $g(\cdot)$  is the function such that  $g(y) = x$  is the solution of  $f(x) = y$  with  $f(x) = x \ln[(1+x)/(1-x)]$ . As  $\sigma^{ss} \rightarrow 0$ , the lower and upper bounds in Eq. (13) go to zero, and hence  $\langle J^{ss} \rangle_a$  correctly vanishes since one tends to equilibrium conditions. As discussed in the Appendix, the inequalities in Eq. (13) become equalities if, again, half of the average recurrence frequencies are equal to  $\bar{\omega}_{\max}$  and the ones of the complementary backward processes are equal to  $\bar{\omega}_{\min}$ . In such a peculiar case the lower and upper bounds do coincide and  $\langle J^{ss} \rangle_a$  is exactly determined (specifically, it is equal to  $\bar{\omega}_{\max} - \bar{\omega}_{\min}$ ).

It is clear that Eqs. (9) and (13) are useful in practice only if  $\langle \bar{\omega} \rangle_a$ ,  $\langle \bar{\omega} \rangle'_a$ , and  $\langle J^{ss} \rangle_a$  can be connected with relevant physical properties. For instance, the utility of Eq. (13) is illustrated later in Sec. IV where, for the continuous case of tilted one-dimensional overdamped rotors, the elaboration of  $\langle J^{ss} \rangle_a$  and  $\langle \bar{\omega} \rangle'_a$  leads to an upper bound on the average rotation frequency at given  $\sigma^{ss}$ .

### B. Kinetic inequalities

Equations (6) and (9) are *upper* bounds on  $\sigma^{ss}$ . On the other hand, the well-known finite-time thermodynamic uncertainty relation (FTTUR) [1,2] sets a *lower* bound on  $\sigma^{ss}$ . By combining these inequalities coming from rather different viewpoints, we can make a ‘‘shortcut’’ obtaining inequalities of a pure kinetic kind since the dissipation rate is used only as a joining link. Let us elaborate this idea.

First, let us briefly recall the FTTUR. Let  $X$  be a physical property that changes by some amount each time a transition occurs (if  $d_{ij}^X$  is such an amount for the generic  $i \rightarrow j$  transition, then  $d_{ji}^X = -d_{ij}^X$  for the reversed one) and let  $\Delta X(t_{\text{obs}})$  be the net variation of  $X$  if the system is observed for a time  $t_{\text{obs}}$

under steady-state conditions. Then  $r_X(t_{\text{obs}}) = [\langle \Delta X(t_{\text{obs}})^2 \rangle - \langle \Delta X(t_{\text{obs}}) \rangle^2] / \langle \Delta X(t_{\text{obs}}) \rangle^2$  is the squared coefficient of variation where  $\langle \cdot \cdot \cdot \rangle$  are ensemble averages (or expectations from the individual-system perspective). In practice,  $r_X(t_{\text{obs}})$  quantifies the relative fluctuations of  $\Delta X(t_{\text{obs}})$  with respect to the mean under steady-state conditions, or we may say the relative *precision* if a precise variation of  $X$  is a target to achieve. With these positions, the FTTUR consists in the lower bound for the average entropy production rate  $\sigma^{ss} \geq 2[t_{\text{obs}} r_X(t_{\text{obs}})]^{-1}$  and expresses the trade-off between the relative precision of the  $X$  variation (the dynamical output) and the required dissipation. Notably, the FTTUR holds for arbitrary  $t_{\text{obs}}$ . For  $t_{\text{obs}} \rightarrow \infty$  one recovers the original basic form [simply the thermodynamic uncertainty relation (TUR)] [15,16] in which the ratio variance over  $2t_{\text{obs}}$  does converge to an effective diffusion coefficient. The FTTUR may tend to saturation in various conditions depending on the specific features of the system and of the property  $X$  of interest (see, for instance, Ref. [17] and references therein).

The combination of the FTTUR with Eq. (6) yields

$$[t_{\text{obs}} r_X(t_{\text{obs}})]^{-1} \leq \frac{N_c}{2} (\bar{\omega}_{\max} - \bar{\omega}_{\min}) \ln\left(\frac{\bar{\omega}_{\max}}{\bar{\omega}_{\min}}\right), \quad (14)$$

while from the combination with Eq. (9) we get

$$[t_{\text{obs}} r_X(t_{\text{obs}})]^{-1} \leq N_c \langle \bar{\omega} \rangle'_a \Phi\left(\frac{\bar{\omega}_{\max}}{\bar{\omega}_{\min}}\right). \quad (15)$$

Equations (14) and (15) give entire families of kinetic inequalities (one per each specific property of interest) of a pure *kinetic* kind. In general, it is expected that such kinetic inequalities are loose order relations since they derive from two bounds on  $\sigma^{ss}$  which, by themselves, are typically loose. Moreover, the  $\leq$  comes from two separate inequalities that are generally saturated under different conditions.

Among the many possible applications, let us focus on the case in which  $\Delta X(t_{\text{obs}}) \equiv n_{ij}(t_{\text{obs}})$  is the net number of transitions (counting the forward and the backward ones and taking the difference) from a site  $i$  to a connected site  $j$  in time  $t_{\text{obs}}$ . The squared coefficient of variation is  $r_{ij}(t_{\text{obs}}) = [\langle n_{ij}(t_{\text{obs}})^2 \rangle - \langle n_{ij}(t_{\text{obs}}) \rangle^2] / \langle n_{ij}(t_{\text{obs}}) \rangle^2$ . Let us consider Eq. (15), which is typically expected to be more stringent than Eq. (14). Such an inequality holds for all pairs of connected sites. In particular, we can write the inequality for the most limiting case corresponding to the lowest of the  $r_{ij}(t_{\text{obs}})$ . This yields

$$\min_{i,j} \{r_{ij}(t_{\text{obs}})\} \geq \left[ N_c \langle \bar{\omega} \rangle'_a t_{\text{obs}} \Phi\left(\frac{\bar{\omega}_{\max}}{\bar{\omega}_{\min}}\right) \right]^{-1}. \quad (16)$$

This inequality tells us that, given the temporal width  $t_{\text{obs}}$ , the relative precision of the net number of jumps from one site to another is limited by the quantity on the right-hand side. Note that such a quantity depends on the temporal width of observation; as  $t_{\text{obs}}$  increases, the right-hand side of Eq. (16) tends to zero and the inequality reduces to the trivial fact that  $r_{ij}(t_{\text{obs}})$  is positive valued.

The relation (16) is illustrated in Fig. 2 for networks with  $N = 3$  sites. The panels contain the same randomly generated instances shown in Fig. 1(a). Given the set of jump rates of each instance, the  $r_{ij}(t_{\text{obs}})$  were obtained [18] from stochas-

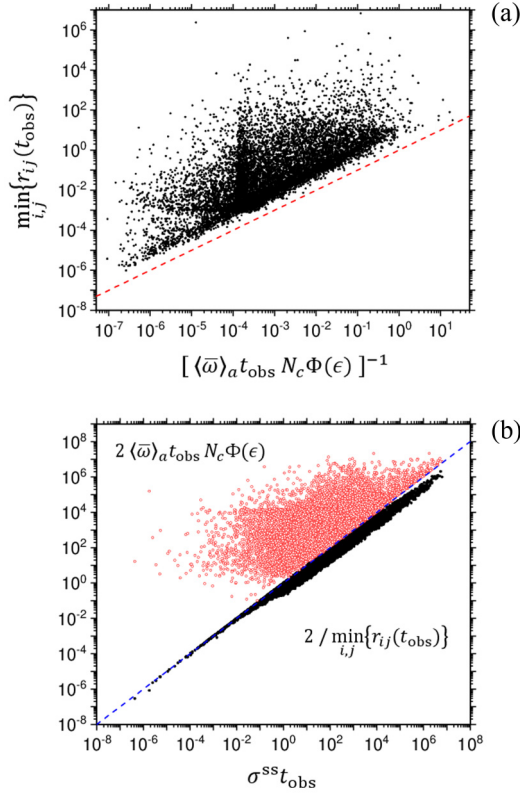


FIG. 2. (a) Effectiveness of the kinetic inequality (16) for the same randomly generated instances of networks with  $N = 3$  sites shown in Fig. 1(a) and for  $t_{\text{obs}} = 10^3$  [14]. (b) Simultaneous check of the FTTUR (points below the line) and of Eq. (9) (points above the line); see the text and Ref. [18] for details. The dashed red lines, of slope 1 and passing through the origin, help to assess the fulfillment of the inequalities.

tic paths simulated with Gillespie's algorithm [19]. The observation time was set equal to  $t_{\text{obs}} = 10^3$ , where the time unit is implicitly fixed by the chosen simulation setup [14]. In Fig. 2(a), the values of  $\min_{i,j}\{r_{ij}(t_{\text{obs}})\}$  are plotted against the values on the right-hand side of Eq. (16). The fulfillment of the inequality is shown by the fact that the points fall above the dashed line of slope 1. For completeness, Fig. 2(b) shows the same data in a way so as to view simultaneously the fulfillment of the FTTUR (points below the line) and of Eq. (9) (points above the line). Note that in this simulation the values of  $\sigma^{\text{ss}}$  span almost eight orders of magnitude. Of course, the filling in Fig. 2(b) is by no means exhaustive and reflects the way in which the network instances have been generated [14].

#### IV. CONTINUOUS DEGREES OF FREEDOM: THE CASE OF DIFFUSION IN TILTED PERIODIC POTENTIALS

Markov processes on discrete state space are sometimes conveniently approximated to continuous processes. A paradigmatic case is the continuous version of stochastic chemical kinetics at different levels of description [20,21]. Conversely, continuous processes can be cast, at least in principle, into Markov jump processes by means of finite-element methods. In both cases one gains some advantage and/or

insight. The latter perspective is of interest here, since once a continuous process is discretized, the results presented above for the discrete case are directly applicable; the return to continuity is then done by taking the limit of elements of vanishing extension.

As example let us focus on overdamped fluctuations of a one-dimensional rotor with constant diffusion coefficient  $D$  and subjected to a constant drift due to a nonconservative tilt  $f > 0$  so that an out-of-equilibrium steady state is sustained. Assume that the evolution of the conditional probability density  $\rho(x, t|x_0)$  on  $x \in [0, 2\pi]$  can be modeled by means of the Fokker-Planck equation  $\partial_t \rho(x, t|x_0) = -\hat{\Gamma} \rho(x, t|x_0)$  with the operator  $\hat{\Gamma} = -D \partial_x \phi(x) \partial_x \phi(x)^{-1}$  in which  $\phi(x) = \exp\{-[V(x) - fx]\}$ , where  $V(x)$  is a periodic function giving the bare energy of the system and  $V(x) - fx$  is the tilted potential; all energies are meant to be expressed in  $k_B T$  units. Such a kind of diffusion in tilted potentials is encountered, for instance, in the modeling of Brownian motors [22]. Recently, tilted periodic potentials have also been employed to get insight into the thermodynamic uncertainty relation in one dimension [23] and two dimensions with coupled degrees of freedom [24].

Let us make a homogeneous partition of the domain into  $N$  small elements of width  $\delta_x = 2\pi/N$ . Each element, with the center at  $x_i = (i - \frac{1}{2})\delta_x$  for  $i = 1, \dots, N$ , constitutes a site. By employing the finite-element approximation scheme with boundary conditions on the probability current at  $x = 0$  and  $x = 2\pi$ , the Fokker-Planck equation turns into the master equation  $\dot{\mathbf{p}} = -\mathbf{R}\mathbf{p}$ , where  $\mathbf{p}(t)$  is the column array whose entries are the site occupation probabilities, i.e.,  $p_i(t) = \rho(x_i, t|x_{i_0})\delta_x$ , and  $\mathbf{R}$  is the  $N \times N$  matrix associated with  $\hat{\Gamma}$ . The element-to-element jump rate is then  $k_{i \rightarrow j} = \lim_{\delta t \rightarrow 0} \{[e^{-\mathbf{R}\delta t}]_{ji}/\delta t\}$ , which gives  $k_{i \rightarrow j} = -R_{ji}$  [25]. As  $N$  increases, the discrete Markov jump process approximates better and better the continuous process. Note that the number of sites (hence connections, since  $N_c^* = N_c = N$  in this case) affects the value of the jump rates through their dependence on  $\delta_x$ . Given the jump rates, the average recurrence times  $\bar{\tau}_{ij}$  (for  $i$  and  $j$  adjacent sites) are computed by means of Eq. (3) and all other required quantities are then obtained.

Direct numerical inspections have led us to see that, for large  $N$ ,  $\sigma^{\text{ss}}$  becomes independent of  $N$  (as expected, since  $\sigma^{\text{ss}}$  is an intrinsic property of the system), whereas the  $\bar{\tau}_{ij}$  are proportional to  $N^{-1}$  and hence the  $\bar{\omega}_{ij}$  are proportional to  $N$ . This implies that the inequalities presented in Sec. III become useless or trivial, with the exception of Eq. (13) (with  $\langle\bar{\omega}\rangle'_a \equiv \langle\bar{\omega}\rangle_a$  in this case), in which the lower bound goes to zero [26] but the upper bound converges as  $N \rightarrow \infty$ . In fact, since the argument of the function  $g$  tends to zero as  $N \rightarrow \infty$  and considering that  $g(y) \simeq \sqrt{y/2}$  for small  $y$ , it follows that  $\langle J^{\text{ss}} \rangle_a \leq \sqrt{\sigma^{\text{ss}} \omega_\infty}$ , where we have introduced the rate  $\omega_\infty = \lim_{N \rightarrow \infty} (\langle\bar{\omega}\rangle_a / N)$  (it is found that  $\langle\bar{\omega}\rangle_a \propto N$  for large  $N$ ; hence the non-null limit does exist). Implicitly, this tells us that  $\langle J^{\text{ss}} \rangle_a$  has a finite limit for  $N \rightarrow \infty$ . This is indeed correct since, for sites connected forming a cycle, all terms  $|J^{\text{ss}}_{i \rightarrow j}|$  in Eq. (12) are equal and correspond to the steady-state probability current which, in the continuum limit, we denote simply by  $J^{\text{ss}}$ . Thus,  $\langle J^{\text{ss}} \rangle_a$  tends to  $J^{\text{ss}}$  as  $N \rightarrow \infty$ .

Let us focus now on the rate  $\omega_\infty$ , which is the crucial parameter. In a series of tests with various forms of the bare

potential  $V(x)$ , also featuring many minima and maxima with large barriers, and for several values of the tilt  $f$ , it was found that  $\langle \bar{\omega} \rangle_a / N$  always tends asymptotically to  $D/(2\pi)^2$  as  $N$  is increased [27]. Thus, it turns out that  $\omega_\infty$  is system independent and we set  $\omega_\infty = D/(2\pi)^2$ . Intuitively, this tells us that  $\omega_\infty$  is determined by the very local back-and-forth motion which is unaffected by the specific features of the tilted potential. In fact, the repetition of the transition from one site to an adjacent one can occur even when the system simply goes one step (or a few steps) back and then moves forward again; on the very local scale (as  $N \rightarrow \infty$ ) the sites are quasiequivalent and the operation of arithmetic mean to get  $\langle \bar{\omega} \rangle_a$  makes a further smoothing. Based on such empirical evidence, we get  $J^{\text{ss}} \leq (2\pi)^{-1} \sqrt{D\sigma^{\text{ss}}}$ . By introducing the average angular velocity of rotation at the steady state (in radians per unit of time), i.e.,  $v = 2\pi J^{\text{ss}}$ , it follows that

$$v \leq \sqrt{D\sigma^{\text{ss}}}. \quad (17)$$

Equation (17) expresses an upper bound on the rotation speed in terms of the average rate of entropy production (dissipation) and of the *microscopic* diffusion coefficient. Although we are dealing with a rotor, basically to help visualize the finite number of sites upon discretization, the result (17) holds also for any unfolded and unrestricted one-dimensional diffusion in a tilted periodic potential. For instance, in the case of translational diffusion,  $v$  becomes the average steady-state linear velocity and  $D$  the microscopic translational diffusion coefficient.

Concerning Eq. (17), we stress that it is a semiempirical result obtained from the observed behavior of  $\langle \bar{\omega} \rangle_a / N$  as  $N \rightarrow \infty$ . On the other hand, the soundness of Eq. (17) is supported by the fact that it can be directly deduced from the FTTUR in the limit of observation time  $t_{\text{obs}}$  finite but vanishingly small. In fact, if the “output” is the displacement  $\Delta x(t_{\text{obs}})$  at the steady state, we have that  $\langle \Delta x(t_{\text{obs}}) \rangle = vt_{\text{obs}}$  and, for  $t_{\text{obs}} \rightarrow 0$ ,  $[\langle \Delta x(t_{\text{obs}})^2 \rangle - \langle \Delta x(t_{\text{obs}}) \rangle^2] / 2t_{\text{obs}} \rightarrow D$  by definition. With these positions, Eq. (17) is exactly the FTTUR for  $t_{\text{obs}} \rightarrow 0$  [28]. This finding is illustrative of how the general relations derived in the discrete setup can be of use to unveil interesting features also for continuous degrees of freedom. In retrospective, Eq. (17) has been derived from the upper bound in Eq. (13) which comes (see the Appendix) from a lower bound on  $\sigma^{\text{ss}}$ , as for the FTTUR.

In passing, we note that Eq. (17) might be a bound tighter than the analogous relation, obtained from the basic TUR ( $t_{\text{obs}} \rightarrow \infty$ ), which is employed in the characterization of the efficiency of molecular motors (see Ref. [15] and the explicit form in Ref. [29], recently discussed also in Ref. [30]). The TUR reads  $v \leq \sqrt{D_{\text{eff}}\sigma^{\text{ss}}}$ , where  $D_{\text{eff}} = \lim_{t_{\text{obs}} \rightarrow \infty} [\langle \Delta x(t_{\text{obs}})^2 \rangle - \langle \Delta x(t_{\text{obs}}) \rangle^2] / 2t_{\text{obs}}$  is the effective diffusion coefficient. Contrary to the microscopic coefficient  $D$ ,  $D_{\text{eff}}$  depends on the features of the bare potential  $V(x)$  and on the applied tilt  $f$ . The methodology for the calculation of  $D_{\text{eff}}$  in tilted periodic potentials has been developed in Ref. [31]. In the case of flat bare potential, the two coefficients coincide for any value of  $f$ . For nonflat potentials,  $D_{\text{eff}} < D$  as  $f \rightarrow 0$ , while for large  $f$  the effective coefficient tends to  $D$  [23]. In the intermediate range,  $D_{\text{eff}}$  may even exceed  $D$  due to resonancelike effects when the applied tilt is close to the

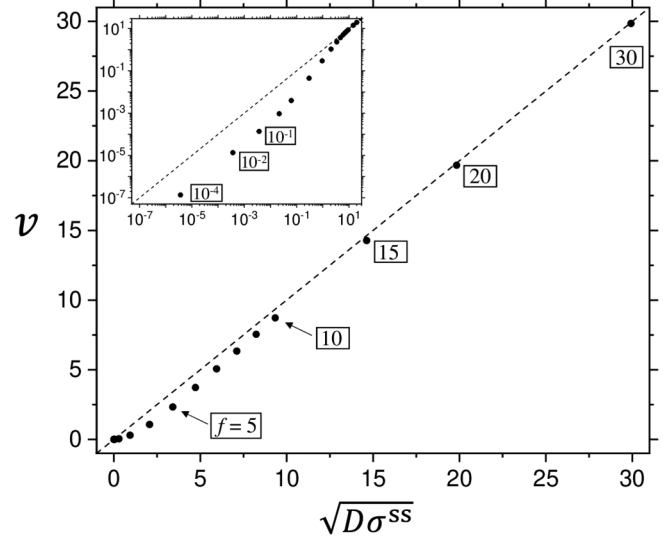


FIG. 3. Effectiveness of the inequality (17) for the overdamped rotor with bare energy  $V(x) = 5 \cos x$  under a constant tilt  $f$  of various magnitudes from  $10^{-4}$  to 30 ( $f$  increases from left to right in the diagram; some values of  $f$  are reported close to the corresponding points). The microscopic diffusion coefficient is set to  $D = 1$ . Energies are expressed in  $k_B T$  units, entropy in  $k_B$  units, and the time in immaterial units. The inset shows the same data in double-logarithmic scale. The dashed lines, of slope 1, help to assess the fulfillment of the inequality.

critical value above which  $V(x) - fx$  becomes a monotonic decreasing function [31]. Thus, Eq. (17) is more stringent than the basic TUR where  $D_{\text{eff}} > D$ . Finally, we also note that Eq. (17) resembles Eq. (8b) of Ref. [32] (based on a previous result by Mazonka and Jarzynski [33]) concerning rotary machines deterministically driven by an external apparatus; when one replaces the average work per cycle (in  $k_B T$  units) at the steady state with the average entropy production (in  $k_B$  units), the two results do coincide. On the other hand, the two contexts are quite different since here the velocity  $v$  is an average quantity because the cycle duration is statistically distributed, not externally controlled.

Figure 3 shows the effectiveness of Eq. (17) for the case  $V(x) = V_0 \cos x$  with  $V_0 = 5$ ,  $D = 1$  (in some units of inverse of time). The rotor’s bare potential features a single well and the rotation is impeded by a barrier of ten units. As  $f$  increases,  $V(x) - fx$  is more and more tilted and, beyond the critical value 5, the energy barrier vanishes. The calculations have been done for several values of  $f$  ranging from  $10^{-4}$  to 30, well above the critical value. For each value of  $f$ , both  $\sigma^{\text{ss}}$  [Eq. (2)] and  $J^{\text{ss}}$  [Eq. (12)] have been computed by using the average recurrence frequencies obtained from the discretized version of the Fokker-Planck equation taking  $N$  larger and larger up to numerical convergence [34]. Note that all points  $v$  vs  $\sqrt{D\sigma^{\text{ss}}}$  lie below the dashed line of slope 1; hence Eq. (17) is fulfilled in the whole range. The inset shows the data in double-logarithmic scale to magnify the details at low values of the tilt. At low tilt, getting closer and closer to equilibrium, the points show a systematic relative deviation from the bound, while it is known that the TUR tends to be saturated in such a limit [23]. This is because  $D_{\text{eff}} < D$  as  $f \rightarrow 0$ , and

hence the bound (17) is less stringent than the TUR. At high tilt it has been shown that the TUR is again saturated [23], and the same happens for Eq. (17) because  $D_{\text{eff}} \simeq D$  in such a limit. In this example, it is found numerically [by means of Eq. (8) of Ref. [23]] that  $D_{\text{eff}}$  reaches the value  $2.7D$  at about the critical tilt, which is where Eq. (17) is slightly more stringent than the TUR.

Similar outcomes have been obtained for other forms of the bare potential  $V(x)$ . In the special case of a flat bare potential, it has been checked that Eq. (17) is an equality for all  $f$ . In fact, this is a case in which the average recurrence frequencies of the forward steps  $i \rightarrow i+1$  are all equal (to  $\omega_{\text{max}}$ ) and also the frequencies of the backward steps  $i \rightarrow i-1$  are all equal (to  $\omega_{\text{min}}$ ); in such a situation the inequalities in Eq. (13) become equalities and the same happens for the derived Eq. (17).

## V. CONCLUSIONS AND PERSPECTIVES

For stationary Markov jump processes on a finite number of sites we have derived inequalities between the average entropy production rate  $\sigma^{\text{ss}}$  and the average recurrence frequencies of the site-to-site transitions. We have also sketched how the results can be extended, at least in principle, to the continuous case.

The inequalities derived here are general and involve a small amount of information about the internal features of the system. The bounds could be tightened by looking more closely at the system's details (e.g., by distinguishing the site-site connections on the basis of their contribution to  $\sigma^{\text{ss}}$ ) but at the price of losing generality and easy interpretation; this is against the spirit of this work. Note that in our derivation we have not used the steady-state constraint requiring that  $\sum_{j \neq i} \bar{\omega}_{ij} = \sum_{j \neq i} \bar{\omega}_{ji}$  for each site  $i$ . The enforcement of such a constraint might lead to tightened bounds and deserves consideration.

The main results are upper bounds on  $\sigma^{\text{ss}}$  [especially Eq. (9)]. The combination of such bounds with the finite-time thermodynamic uncertainty relation, a lower bound on  $\sigma^{\text{ss}}$ , yields inequalities of a pure kinetic kind [Eqs. (14) and (15)] for the relative precision of an output. Individuating the possible conditions under which such kinetic inequalities may be saturated requires further insight.

Concerning the continuous processes, the one-dimensional case treated here shows how the bounds derived for the discrete case can be of use in allowing interesting inequalities to emerge in the continuous case [like Eq. (17)], which is equivalent to the finite-time TUR in the limit  $t_{\text{obs}} \rightarrow 0$ . It would be interesting now to explore more complex high-dimensional situations.

## APPENDIX: PROOFS

Let us introduce the factors  $\epsilon_{ij} = \bar{\tau}_{ij}/\bar{\tau}_{ji} = \bar{\omega}_{ji}/\bar{\omega}_{ij}$ . The conditions  $\epsilon_{ij} > 1$  and  $\epsilon_{ij} < 1$  separate the site-to-site transitions contributing to  $\sigma^{\text{ss}}$  in two sets indicated below by the arrows  $\uparrow$  and  $\downarrow$ , respectively. Let us introduce the notation for restricted summations over such sets:

$$\sum_{j \neq i}^{\uparrow} \equiv \sum_{j \neq i, \epsilon_{ij} > 1}, \quad \sum_{j \neq i}^{\downarrow} \equiv \sum_{j \neq i, \epsilon_{ij} < 1}. \quad (\text{A1})$$

The primed summations  $\sum'_{j \neq i}$  will denote sums over both sets. Then let us introduce

$$S = \sum_i \sum_{j \neq i}^{\uparrow} \bar{\omega}_{ij}, \quad H = \sum_i \sum_{j \neq i}^{\downarrow} \bar{\omega}_{ij}. \quad (\text{A2})$$

Now we consider the set of transitions selected by  $\epsilon_{ij} > 1$  and introduce  $\alpha_i = S^{-1} \sum_{j \neq i}^{\uparrow} \bar{\omega}_{ij}$  (with  $\sum_i \alpha_i = 1$ ) and  $\rho_j^{(i)} = \bar{\omega}_{ij} / \sum_{j \neq i}^{\uparrow} \bar{\omega}_{ij}$  (with  $\sum_{j \neq i}^{\uparrow} \rho_j^{(i)} = 1$  for all  $i$ ). With these positions,  $\sigma^{\text{ss}}$  in Eq. (2) can be written as

$$\sigma^{\text{ss}} = S \sum_i \alpha_i \sum_{j \neq i}^{\uparrow} \rho_j^{(i)} F(\epsilon_{ij}), \quad (\text{A3})$$

where we have introduced the function

$$F(x) = (x-1) \ln x \quad (\text{A4})$$

for  $x > 0$ . Such a function is non-negative (it vanishes only at  $x = 1$ ) and convex. By construction, the  $\alpha_i > 0$  and the  $\rho_j^{(i)} > 0$  behave as if they were ‘‘probabilities’’ over their own sets. By exploiting the convexity of  $F$  and applying Jensen's inequality two times we have

$$\begin{aligned} \sigma^{\text{ss}} &\geq S \sum_i \alpha_i F\left(\sum_{j \neq i}^{\uparrow} \rho_j^{(i)} \epsilon_{ij}\right) \\ &\geq S F\left(\sum_i \sum_{j \neq i}^{\uparrow} \alpha_i \rho_j^{(i)} \epsilon_{ij}\right). \end{aligned} \quad (\text{A5})$$

By recalling the definitions given above and considering that  $\sum_i \sum_{j \neq i}^{\uparrow} \bar{\omega}_{ji} \equiv \sum_i \sum_{j \neq i}^{\downarrow} \bar{\omega}_{ij} = H$ , the argument of  $F$  in the last line corresponds to  $H/S$ . Thus,

$$\sigma^{\text{ss}} \geq S F\left(\frac{H}{S}\right). \quad (\text{A6})$$

With a similar derivation, but operating with the set of transitions selected by  $\epsilon_{ij} < 1$ , we arrive at

$$\sigma^{\text{ss}} \geq H F\left(\frac{S}{H}\right). \quad (\text{A7})$$

Let us now introduce  $\Omega = H + S$  and  $\Delta = H - S$ , which can be expressed as

$$\Omega = \sum_i \sum_{j \neq i}^{\uparrow} \bar{\omega}_{ij}, \quad \Delta = \sum_i \sum_{j < i} |\bar{\omega}_{ji} - \bar{\omega}_{ij}|. \quad (\text{A8})$$

By writing  $S = (\Omega - \Delta)/2$  and  $H = (\Omega + \Delta)/2$  and introducing the ratio  $r = \Delta/\Omega$ , both Eqs. (A6) and (A7) yield the same inequality

$$\frac{\sigma^{\text{ss}}}{\Omega} \geq f(r), \quad (\text{A9})$$

where we have introduced the function

$$f(x) = x \ln \left( \frac{1+x}{1-x} \right). \quad (\text{A10})$$

Since  $f(x)$  is monotonically increasing, we get an upper bound on  $r$  at given  $\sigma^{\text{ss}}/\Omega$ . Ultimately, we arrive at the inequality which sets an upper bound on  $\Delta$ ,

$$\Delta \leq \Omega g\left(\frac{\sigma^{\text{ss}}}{\Omega}\right), \quad (\text{A11})$$

where  $g(\cdot)$  is the inverse function such that  $g(y) = x$  is the solution of  $f(x) = y$ . We see that  $g(0) = 0$  and  $g$  monotonically increases with limit 1. Note that in the peculiar case in which half of the average recurrence frequencies are equal to  $\bar{\omega}_{\max}$  and the ones for the complementary backward processes are equal to  $\bar{\omega}_{\min}$ , both Eqs. (A6) and (A7) become equalities and equivalent to each other [and also equivalent to Eq. (6) with the equality, when  $N_c$  is replaced by  $N_c^*$ ]. In such a case, also the final equation (A11) is saturated.

From a different angle we get a majorization of  $\sigma^{\text{ss}}$ :

$$\begin{aligned} \sigma^{\text{ss}} &= \sum_i \sum_{j<i} |\bar{\omega}_{ji} - \bar{\omega}_{ij}| \left| \ln \frac{\bar{\omega}_{ji}}{\bar{\omega}_{ij}} \right| \\ &\leq \Delta \ln \frac{\bar{\omega}_{\max}}{\bar{\omega}_{\min}}. \end{aligned} \quad (\text{A12})$$

Such a majorization is the critical step since the inequality can be saturated, as for Eq. (A11), only if all connections are nonbalanced and half of the transitions have average recurrence frequencies all equal to  $\bar{\omega}_{\max}$ , while the associated backward transitions have frequencies equal to  $\bar{\omega}_{\min}$ . By coupling Eq. (A12) with (A11) we get  $\sigma^{\text{ss}} \leq \Omega g(\sigma^{\text{ss}}/\Omega) \ln(\bar{\omega}_{\max}/\bar{\omega}_{\min})$ , which can be written as

$$\mathcal{L}(\sigma^{\text{ss}}/\Omega) \leq \ln \left( \frac{\bar{\omega}_{\max}}{\bar{\omega}_{\min}} \right), \quad (\text{A13})$$

with the function

$$\mathcal{L}(x) = \frac{x}{g(x)} \equiv \ln \left[ \frac{1+g(x)}{1-g(x)} \right]. \quad (\text{A14})$$

Since the logarithm is a monotonically increasing function, it follows that  $[1 + g(\sigma^{\text{ss}}/\Omega)]/[1 - g(\sigma^{\text{ss}}/\Omega)] \leq \epsilon$  with  $\epsilon = \bar{\omega}_{\max}/\bar{\omega}_{\min}$ ; thus

$$g\left(\frac{\sigma^{\text{ss}}}{\Omega}\right) \leq \frac{\epsilon - 1}{\epsilon + 1}. \quad (\text{A15})$$

The same order relation holds when we evaluate the function  $f(\cdot)$  [Eq. (A10)] on both sides of Eq. (A15). By definition,  $f(g(\sigma^{\text{ss}}/\Omega)) = \sigma^{\text{ss}}/\Omega$  from the left-hand side, while from the right-hand side we get  $[(\epsilon - 1)/(\epsilon + 1)] \ln \epsilon$ . By introducing  $\langle \bar{\omega} \rangle'_a = \Omega/2N_c^*$ , i.e., the analog of the mean frequency defined in Eq. (11) but evaluated only over the nonbalanced connections, it follows that

$$\sigma^{\text{ss}} \leq 2N_c^* \langle \bar{\omega} \rangle'_a \left( \frac{\epsilon - 1}{\epsilon + 1} \right) \ln \epsilon, \quad (\text{A16})$$

which extends Eq. (9). The relation (9) is finally obtained as a majorization once  $N_c^* \langle \bar{\omega} \rangle'_a \leq N_c \langle \bar{\omega} \rangle_a$  is considered.

Concerning the mean current defined in Eq. (12), the bounds given in Eq. (13) readily follow by considering that  $\langle J^{\text{ss}} \rangle_a \equiv \Delta/N_c^*$  and employing the upper bound [Eq. (A11)] and the lower bound [from Eq. (A12)] on  $\Delta$ . Under the peculiar conditions for which Eqs. (A11) and (A12) are (both) saturated as indicated above, the lower and upper bounds in Eq. (13) do coincide and hence  $\langle J^{\text{ss}} \rangle_a$  is exactly determined.

- 
- [1] P. Pietzonka, F. Ritort, and U. Seifert, Finite-time generalization of the thermodynamic uncertainty relation, *Phys. Rev. E* **96**, 012101 (2017).
- [2] J. M. Horowitz and T. R. Gingrich, Proof of the finite-time thermodynamic uncertainty relation for steady-state currents, *Phys. Rev. E* **96**, 020103(R) (2017).
- [3] G. Falasco and M. Esposito, Dissipation-Time Uncertainty Relation, *Phys. Rev. Lett.* **125**, 120604 (2020).
- [4] J. Schnakenberg, Network theory of microscopic and macroscopic behavior of master equation systems, *Rev. Mod. Phys.* **48**, 571 (1976).
- [5] D. Frezzato, Stationary Markov jump processes in terms of average transition times: Setup and some inequalities of kinetic and thermodynamic kind, *J. Phys. A: Math. Theor.* **53**, 365003 (2020).
- [6] D. Frezzato, Sensitivity analysis of the reaction occurrence and recurrence times in steady-state biochemical networks, *Math. Biosci.* **332**, 108518 (2021).
- [7] B. E. Husic and V. S. Pande, Markov state models: From an art to a science, *J. Am. Chem. Soc.* **140**, 2386 (2018).
- [8] A. B. Kolomeisky and M. E. Fisher, Molecular motors: A theorist's perspective, *Annu. Rev. Phys. Chem.* **58**, 675 (2007).
- [9] J. Shin and A. B. Kolomeisky, Asymmetry of forward/backward transition times as a non-equilibrium measure of complexity of microscopic mechanisms, *J. Chem. Phys.* **153**, 124103 (2020).
- [10] D. T. Gillespie, Stochastic simulation of chemical kinetics, *Annu. Rev. Phys. Chem.* **58**, 35 (2007).
- [11] A. Sabatino and D. Frezzato, Tagged-moiety viewpoint of chemical reaction networks, *J. Chem. Phys.* **150**, 134104 (2019).
- [12] A. Sabatino, E. Penocchio, G. Ragazzon, A. Credi, and D. Frezzato, Individual-molecule perspective analysis of chemical reaction networks: The case of a light-driven supramolecular pump, *Angew. Chem. Int. Ed.* **58**, 14341 (2019).
- [13] If one prefers to deal with the timing of the recurrences, all expressions can be rewritten in terms of the harmonic mean time  $\langle \bar{\tau} \rangle_h \equiv \langle \bar{\omega} \rangle_a^{-1}$ .
- [14] In the simulations, the value  $k_{1 \rightarrow 2} = 1$  was adopted to fix the scale. The other jump rates were assigned by setting  $k_{i \rightarrow j} = 10^{u_{ij}}$  with  $u_{ij}$  randomly drawn from the uniform distribution between  $-4$  and  $+4$ . For each set of jump rates, the average recurrence times for all site-to-site transitions were computed by means of Eq. (3); then, the extrema  $\bar{\tau}_{\max}$  and  $\bar{\tau}_{\min}$  [hence  $\bar{\omega}_{\max}$  and  $\bar{\omega}_{\min}$  required in Eq. (9)] were individuated according to Eq. (4).
- [15] A. C. Barato and U. Seifert, Thermodynamic Uncertainty Relation for Biomolecular Processes, *Phys. Rev. Lett.* **114**, 158101 (2015).
- [16] T. R. Gingrich, J. M. Horowitz, N. Perunov, and J. L. England, Dissipation Bounds All Steady-State Current Fluctuations, *Phys. Rev. Lett.* **116**, 120601 (2016).



- [17] S. K. Manikandan, D. Gupta, and S. Krishnamurthy, Inferring Entropy Production from Short Experiments, *Phys. Rev. Lett.* **124**, 120603 (2020).
- [18] For each stochastic path, the initial site was sampled at random using the steady-state occupation probabilities as weight factors. Up to time  $t_{\text{obs}}$ , for all connected pairs  $i$  and  $j$  the net numbers of transitions from  $i$  to  $j$  were counted; the averages  $\langle n_{ij}(t_{\text{obs}}) \rangle$  and  $\langle n_{ij}(t_{\text{obs}})^2 \rangle$  were determined over  $N_{\text{sim}}$  simulated paths. As a requirement of statistical quality it was imposed that the global relative deviation of the  $\langle n_{ij}(t_{\text{obs}}) \rangle$  from the exact values was at most 2% (the global relative deviation was taken as the root mean of the squared relative deviations). In most cases,  $N_{\text{sim}} = 10^4$  ensured a global deviation below 0.1%. Otherwise,  $N_{\text{sim}}$  was iteratively increased by a factor 10 to bring the deviation below 2%. In the few critical cases in which the FTTUR was apparently violated (though very slightly) because of poor statistics,  $N_{\text{sim}}$  was further increased to lower the deviation below 1%; then the outcome was accepted in any case.
- [19] D. A. Gillespie, A general method for numerically simulating the stochastic time evolution of coupled chemical reactions, *J. Comput. Phys.* **22**, 403 (1976).
- [20] D. T. Gillespie, The chemical Langevin equation, *J. Phys. Chem.* **113**, 297 (2000).
- [21] A. Ceccato and D. Frezzato, Remarks on the chemical Fokker-Planck and Langevin equations: Nonphysical currents at equilibrium, *J. Chem. Phys.* **148**, 064114 (2018).
- [22] P. Reinmann and P. Hänggi, Introduction to the physics of Brownian motors, *Appl. Phys. A* **75**, 169 (2002).
- [23] C. Hyeon and W. Hwang, Physical insight into the thermodynamic uncertainty relation using Brownian motion in tilted periodic potentials, *Phys. Rev. E* **96**, 012156 (2017).
- [24] M. W. Jack, N. J. López-Alamilla, and K. J. Challis, Thermodynamic uncertainty relations and molecular-scale energy conversion, *Phys. Rev. E* **101**, 062123 (2020).
- [25] Explicitly,  $k_{i \rightarrow i+1} = D\delta_x^{-2}\phi(x_i)^{-1}\phi(x_i + \delta_x/2)$ ,  $k_{i \rightarrow i-1} = D\delta_x^{-2}\phi(x_i)^{-1}\phi(x_i - \delta_x/2)$ ,  $k_{1 \rightarrow N} = D\delta_x^{-2}\phi(x_N + \delta_x)^{-1}\phi(x_N + \delta_x/2)$ , and  $k_{N \rightarrow 1} = D\delta_x^{-2}\phi(x_1 - \delta_x)^{-1}\phi(x_1 - \delta_x/2)$ .
- [26] Direct numerical inspections made with several forms of  $V(x)$  and values of  $f$  have shown that  $N \ln[\bar{\omega}_{\text{max}}/\bar{\omega}_{\text{min}}]$  [the denominator in the lower bound of Eq. (13)] increases linearly with  $N$  as  $A + BN$ , where  $A$  and  $B$  are case-dependent parameters. As  $N \rightarrow \infty$ , the lower bound in Eq. (13) goes to zero. The exception is found for flat bare energetics, say,  $V(x) = 0$ , for which the  $N$  dependence is lost ( $B = 0$ ) and  $A = 2\pi f$ ; in such a case the lower bound in Eq. (13) takes a finite value and coincides with the upper bound (in fact, this is a case in which the two bounds do coincide and  $\langle J^{\text{ss}} \rangle_a$  is exactly determined).
- [27] Specifically, the deviation of  $\langle \bar{\omega} \rangle_a / N$  from  $D/(2\pi)^2$  asymptotically decreases proportionally to  $N^{-2}$  with a proportionality factor mainly controlled by  $f$ . For example, for the case  $V(x) = 5 \cos(x)$  illustrated here, it was found that with  $N = 400$  intervals the deviation is only 0.6% for  $f = 5$  and 1.2% for  $f = 20$ . The exact numerical equality with  $D/(2\pi)^2$ , even for small  $N$ , is found for unbiased free rotational diffusion.
- [28] We also point out that Eq. (17) differs from the general dissipation-time uncertainty relation of Ref. [3] which in our notation would give an upper bound on  $v$  which is proportional to  $\sigma^{\text{ss}}$ , not on the square root. On the other hand, that relation would be applicable only for  $f$  (and hence  $\sigma^{\text{ss}}$ ) sufficiently large that the inverse cycling is “exponentially rarer” than the direct cycling; in that range, the relation of Ref. [3] is likely a safe majorization of Eq. (17).
- [29] P. Pietzonka, A. C. Barato, and U. Seifert, Universal bound on the efficiency of molecular motors, *J. Stat. Mech.* (2016) 124004.
- [30] C.-B. Li and L. Toyabe, Efficiencies of molecular motors: A comprehensible overview, *Biophys. Rev.* **12**, 419 (2020).
- [31] P. Reinmann, C. Van den Broeck, H. Linke, P. Hänggi, J. M. Rubi, and A. Pérez-Madrid, Diffusion in tilted periodic potentials: Enhancement, universality, and scaling, *Phys. Rev. E* **65**, 031104 (2002).
- [32] A. K. S. Kasper and D. A. Sivak, Modeling work-speed-accuracy trade-offs in a stochastic rotary machine, *Phys. Rev. E* **101**, 032110 (2020).
- [33] O. Mazonka and C. Jarzynski, Exactly solvable model illustrating far-from-equilibrium predictions, [arXiv:cond-mat/9912121](https://arxiv.org/abs/cond-mat/9912121).
- [34]  $N = 200$  was sufficient up to  $f = 20$ ; then  $N$  was taken larger. The numerical fulfillment of some known exact relations was also verified for a cross-check. Specifically, given  $V(x)$  and  $f$ , it has been verified that  $\sigma^{\text{ss}} = vf$  and that  $J^{\text{ss}}$  coincides with the available analytical solution [see Eq. (16) of Ref. [23]].